A Coupled Model Study of Glacial Asian Monsoon Variability and Indian Ocean Dipole

Xiaodong LIU

SKLLQG, Institute of Earth Environment, Chinese Academy of Sciences, Xi'an, China

Zhengyu LIU

Center for Climatic Research, University of Wisconsin-Madison, Madison, Wisconsin, USA

S. CLEMENS, W. PRELL

Department of Geosciences, Brown University, Providence, Rhode Island, USA

and

J. KUTZBACH

Center for Climatic Research, University of Wisconsin-Madison, Madison, Wisconsin, USA

(Manuscript received 4 November 2005, in final form 7 September 2006)

Abstract

A coupled climate model is used to study the response of interannual variability of Asian summer monsoon, and its relation with tropical climate variability over the Pacific and Indian Oceans. Two simulations are performed, one for the present and the other for the Last Glacial Maximum. It is found that at glacial times, the weakened Asian monsoon climatology results in a significant shallowing of mean tropical thermocline in the central-western Indian Ocean. This shallower thermocline intensifies the positive ocean-atmosphere feedback in the western Indian Ocean, and therefore contributes to an enhanced Indian Ocean Dipole (IOP) variability. The increased IOD variability in turn exerts a stronger affect on the variability of South Asian monsoon rainfall, and therefore may have contributed to a significant reduction of correlation between the monsoon and the Pacific El Niño/Southern Oscillation (ENSO) variability.

1. Introduction

The Asian monsoon exhibits strong interannual variability (Webster et al. 1998). A substantial part of the South Asian monsoon variability is known to be associated with the remote tropical Pacific climate variability, notably El Niño/Southern Oscillation (ENSO) (e.g., Shukla and Paolino 1983; Ju and Slingo 1995). During an El Niño event, sea surface temperature (SST) increases in the central-eastern equatorial Pacific, which shifts the deep convection center from the Maritime continent eastward into the central Pacific, reducing rainfall over the western Pacific and South Asia

Corresponding author: Zhengyu Liu, Center for Climatic Research, 1225 W. Dayton St., Madison, WI 53706, U.S.A.
E-mail: zliu3@wisc.edu

(e.g., Latif et al. 2001). As a result, South Asian monsoon rainfall tends to be negatively correlated with the eastern Pacific SST (Shukla 1987).

Recent studies further suggest a substantial impact on the Asian monsoon variability from local climate variability over the tropical Indian Ocean (Ashok et al. 2001; Li et al. 2003), notably the Indian Ocean Dipole (IOD) (Saji et al. 1999; Webster et al. 1999). During a positive IOD phase, the SST anomaly in the tropical Indian Ocean is negative in the east, and positive in the west; this SST gradient forces an anomalous southerly monsoon wind over the northern Indian Ocean, which penetrates into the South Asian continent and enhances rainfall there (Guan et al. 2003; Li et al. 2003; Ashok et al. 2004). This tends to result in a positive correlation between the South Asian rainfall and IOD, which could then distort the correlation between the Asian monsoon and ENSO significantly (Webster et al. 1999; Ashok et al. 2001; Wu and Kirtman 2004). These studies suggest that the South Asian monsoon can be affected significantly by both ENSO and IOD (Ashok et al. 2004). In the mean time, these variability modes (ENSO and IOD) also interact with each other. Observational, and modeling studies suggest that substantial IOD events can be excited by ENSO (Allan et al. 2001; Baquero-Bernal et al. 2002). On the other hand, there are also convincing evidences that a significant number of IOD events are generated locally in the Indian Ocean climate system, independent of the remote Pacific ENSO (Ashok et al. 2003; Saji and Yamagata 2003; Lau and Nath 2004). Some studies also suggest an impact of IOD on ENSO (Behera and Yamagata 2003). All these studies therefore suggested a complex relationship between the South Asian monsoon and the two tropical climate variability modes, the ENSO and the IOD. There are evidences that these relationships are non-stationary, and could change dramatically over interdecadal times. For example, the negative correlation between the Indian monsoon rainfall and Nino3 (averaged for 150°–90°W, 5°S–5°N) SST decreases dramatically after the 1980s (Kumar et al. 1999; Krishnamurthy and Goswami 2000), when the correlation between the Indian summer rainfall and IOD increases significantly (Ashok et al. 2001).

Given the complex and changing relationship between the South Asian monsoon variation and tropical climate variability modes, it is natural to wonder if the relationship has changed in the past, and how it will change in the future, under different climate forcing. This note is motivated by a curiosity if the covariability between the Asian monsoon variability, and tropical climate modes at glacial times differs from the present. Due to the lack of observations on this covariability at glacial periods, we have chosen to explore this issue in a coupled climate model. Our major finding is that, during glacial time, the relationship between the South Asian monsoon and ENSO is reduced significantly, while its correlation with IOD is increased significantly. This occurs, partly, because the reduced Asian monsoon at glacial times changes the tropical Indian Ocean thermocline, which in turn enhances the IOD variability, and in turn its impact on the Asian monsoon.

2. The model

A fully coupled ocean-atmosphere model is used, the Fast Ocean Atmosphere Model (FOAM, Jacob 1997). The AGCM has a resolution of R15 (7.5° long., 4.8° lat., 18 levels). For this study, the OGCM takes the resolution of 2.8° (long.), 1.4° (lat.), and 32 levels (Liu and Yang 2003). Without flux adjustment, FOAM simulates a reasonable tropical climatology, comparable with, for example, the NCAR CCSM1 (Liu et al. 2003). The enhanced Asian monsoon to Holocene climate forcing in FOAM has also been found to be largely consistent with CCSM1 and other models, as well as proxy evidences (Liu et al. 2003; Zhao et al. 2005).

To examine the change of Asian monsoon variability, and its relation with tropical climate variability at glacial times, we performed two 400-year simulations. The present-day climate is simulated in a control run (CTRL), which is forced by the preindustrial climate forcing with an atmospheric CO_2 level of 280 ppm (Hereafter, "present" climate refers to the condition of the preindustrial CO_2 level). The glacial climate is simulated in a glacial run (LGM), which uses the climate forcing at the Last Glacial Maximum, with the continental ice boundary prescribed as the ICE-5G (Peltier

2004), and the atmospheric CO_2 level reduced to 180 ppm. All other conditions, including the land-sea distribution, are identical to those in CTRL. The LGM run is integrated for 400 years, starting from the end of the CTRL. The global surface air temperature decreases rapidly for about 3°C in the first 200 years, with the climate in the last 200 years reaching a quasi-equilibrium state (tropical mean surface air temperature trend of 0.12°C/200-yr). Here, the last 200 years of the CTRL, and LGM runs, will be used for analyses.

Finally, we caution that this study mainly focuses on the change of variability in the FOAM model. As in all other models, FOAM has its deficiencies, such as a weaker ENSO that is perhaps related to the too diffusive thermocline in the coarse resolution model. Therefore, we need to be cautious about the application of the FOAM results to the real world. In the mean time, we also point out that our current understanding of the change of climate variability remains poor, even for ENSO—the most studied variability. As Latif et al. (2001) shows, there is no clear relationship between a model resolution, or a particular physical pameterization, and the realism of the simulated ENSO. One should not be surprised that similar situation occurs for the IOD. Therefore, our study based on FOAM is a useful attempt, in spite of the model deficiencies.

3. Monsoon variability, IOD and ENSO at present

For the present climate, FOAM simulates a reasonable ENSO variability, with the SST variability centered in the central-eastern equatorial Pacific; the dominant period of variability is about 3–4 years (Liu et al. 2000). In the mean time, FOAM also simulates IOD-like variability in the Indian Ocean. Since IOD has not been discussed for FOAM, it will be described in more details here in CTRL. The dipole SST pattern is seen clearly in the EOF2 of monthly SST anomaly over the tropical Indian Ocean (Fig. 1a), which exhibits a strong negative anomaly in the east, and a broad warm anomaly in the west, similar to the observation (Saji et al. 1999; Allan et al. 2001; Behera et al. 2003) (The EOF1 shows a monopole pattern, also consistent with the observation [not shown]). Further features of the IOD can

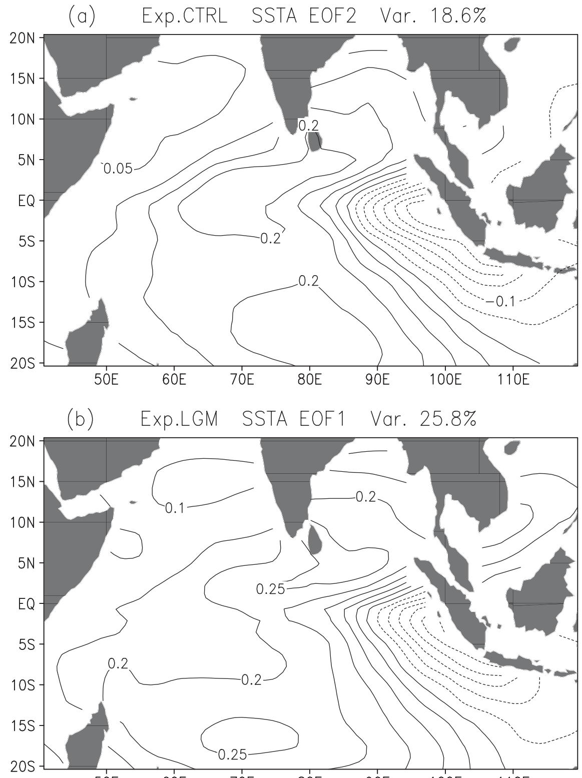

Fig. 1. Model IOD SST patterns for (a) CTRL (EOF2) and (b) LGM (EOF1).

be seen in a composite analysis. Considering the fact that the IOD phenomena mostly appear in boreal summer seasons, a season-based IOD event is defined as an anomalous June–September (JJAS) averaged IOD index, exceeding 0.5 standard deviation, in order to quantificationally reflect the intensity of IOD in each year. The IOD index is the SST difference between the western (60°–80°E, 10°S–10°N) and eastern (90°–110°E, 10°S–0°) Indian Ocean as defined by Saji et al. (1999). The composite is done as the difference of the 25 strongest positive IOD events, and the 25 strongest negative IOD events. The pattern of the composite SST anomaly pattern (not shown) is similar to the EOF in Fig. 1a. The accompanied surface wind and precipitation anomalies of the IOD composites show an easterly over the equator, and an overall northward wind convergence, and in turn an enhanced monsoon rainfall over the western tropical Indian Ocean, India and Southeast Asia (Fig. 2a), and reduced rainfall

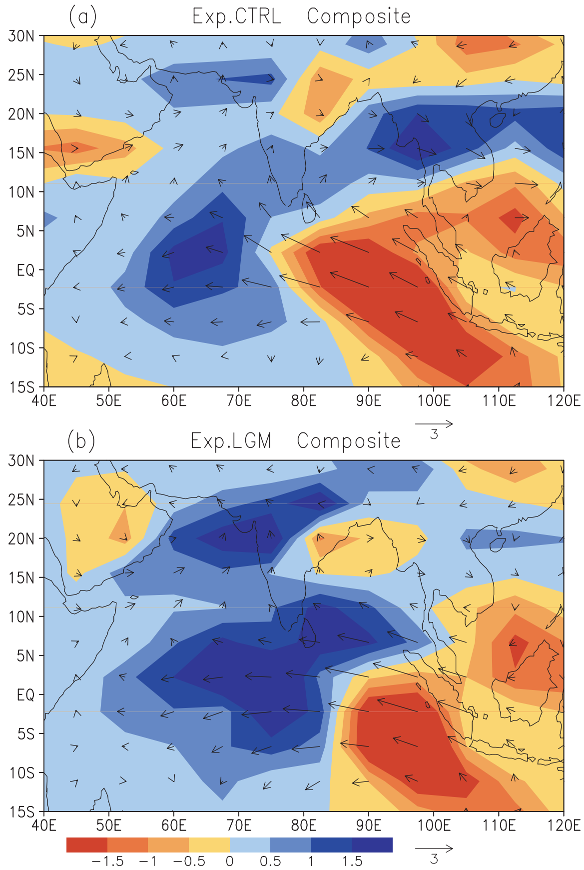

Fig. 2. Composite of IOD events of JJAS precipitation rate (shaded, mm/day) and surface wind (vector, m/s) for (a) CTRL and (b) LGM. The composite is made as the difference of 25 positive IOD events minus 25 negative IOD events.

over the eastern tropical Indian Ocean, largely consistent with the observation (Ashok et al. 2004). The present dipole anomaly extends deep into the thermocline (Fig. 3a), also consistent with the observation (Tokinaga and Tanimoto 2004).

The simulated IOD also exhibits a seasonal phase-locking, with the peak month of SST anomaly occurring in later summer to early fall. Figure 4a shows the monthly evolution of the composite SST anomaly difference centered at the peak year of each IOD event. The anomalous SST, and equatorial zonal wind emerge in late spring, and peak in July to August. The peak IOD month is also consistent with the peak frequency month in summer for all the IOD events (defined as the magnitude of monthly IOD index larger than 0.3°C lasting for at least five months) (light bars in Fig. 5). This phase-locking of the peak IOD is similar to the observation (Saji et al. 1999), although the peak timing is 1–2 months earlier than in the observation[1].

In CTRL, the model Asian monsoon is (negatively) correlated with ENSO statistically significantly (Table 1). Here, the monsoon index is chosen as the JJAS rainfall averaged over land in the region of 65°–105°E and 5°–27°N as defined by Wang et al. (2003). This correlation is comparable with the (positive) monsoon correlation with the IOD (Table 1). The monsoon exhibits an even stronger (negative) correlation with the equatorial zonal wind anomaly. These correlations are generally consistent with the observations (Ashok et al. 2001; Saji and Yamagata 2003).

4. Monsoon co-variability with ENSO and IOD at glacial times

In the LGM simulation, the overall Asian monsoon rainfall over land is generally reduced. The mean surface monsoon wind is also reduced (Fig. 6). This reduction is partly caused by the reduced global hydrological cycle in a colder climate. It is also caused by a reduced land-sea temperature contrast in summer. The summer surface air temperature decreases by over 4°C over the Asian tropical-subtropical continents, while the tropical SST over the

1 The model IOD evolution also exhibits less quasi-biannual oscillation features than in the observation. For example, the model IOD index is near zero in the year preceding the IOD event, while in the observation, for all the IOD events, the IOD index in the preceding year tends to be weakly negative (Saji et al. 1999; Li et al. 2003). Nevertheless, this lack of negative peak in the preceding year is similar to the composite of those IOD events that are not affected by ENSO as in the observation (Saji and Yamagata 2003), and in a model study (Baquero-Bernal et al. 2002). Therefore, the lack of quasi-biannual oscillation feature of the IOD in FOAM, we speculate, is due to the somewhat weaker correlation of ENSO with Indian Ocean SST in FOAM than in the observation (the correlation between Nino3 and Indian Ocean SST is about 0.3 in the model, but about 0.6 in the observation). Dynamically, the model IOD is therefore more like to be stochastic-driven, rather than ENSO-driven (Baquero-Bernal et al. 2002; Li et al. 2003).

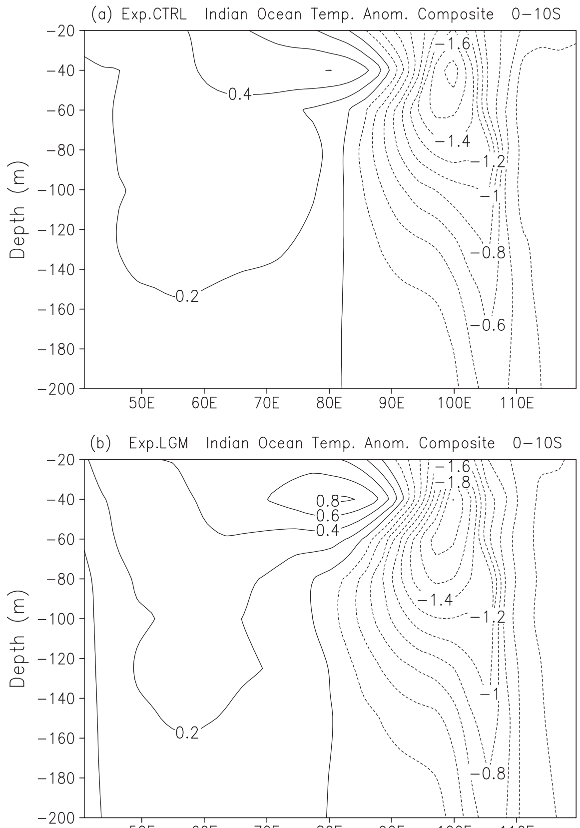

Fig. 3. Composite of IOD events, the same as Fig. 2, but for subsurface ocean temperature anomaly (°C), averaged for 0°–10°S.

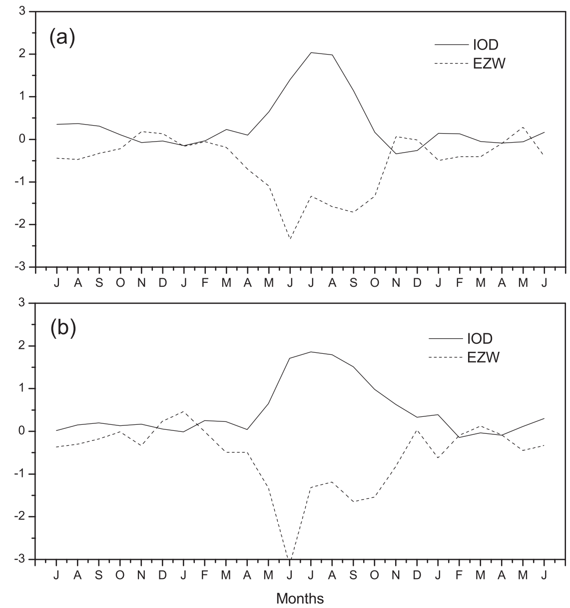

Fig. 4. Monthly differences of the IOD index (solid) and equatorial zonal wind anomaly (dash), averaged for 25 positive IOD events with those for 25 negative IOD events in (a) CTRL and (b) LGM.

Indian Ocean decreases by less than 2°C. This overall reduction of monsoon activity is consistent with previous model simulations (e.g., Kutzbach and Guetter 1986; Dong and Valdes 1998; Shin et al. 2003) as well as proxy evidences (e.g., Anderson and Prell 1993; An et al. 1991). The interannual variance of Asian monsoon rainfall is also weakened by 13%. This reduction is also likely to be related to the reduced hydrological cycle, latent heat release, and in turn monsoon variability, in an overall colder glacial climate.

Most interesting to us here is a dramatic reduction of the correlation between the Asian monsoon rainfall variability and ENSO, with the correlation reduced from −0.22 to a statistically insignificant −0.05 (Table 1). At the same time, the correlations of the monsoon rainfall with IOD and Indian Ocean equatorial zonal

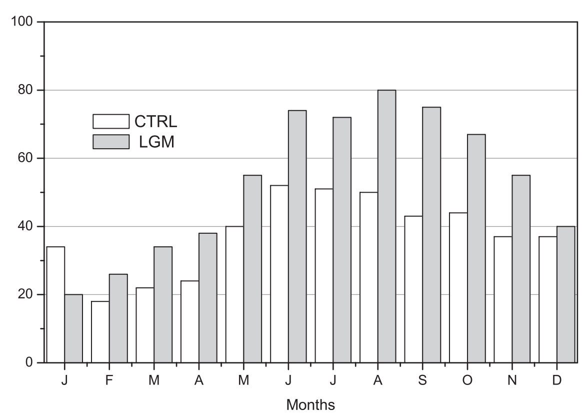

Fig. 5. Occurring months for all the IOD events (defined as the magnitude of IOD index larger than 0.3°C lasting for at least five months) in CTRL and LGM.

Table 1. Correlations between Asian monsoon rainfall (Monsoon) and ENSO (Nino3 SSTA), IOD (IOD index), and equatorial Indian Ocean zonal wind anomaly (EIOZWA, average in 70°–90°E, 5°S–5°N) (Bold numbers indicate correlations exceeding the 99% confidence level for 200 years).

	Nino3 SSTA		IOD Index		EIOZWA	
	CTRL	LGM	CTRL	LGM	CTRL	LGM
Monsoon	**−0.22**	−0.05	**0.26**	**0.37**	**−0.40**	**−0.48**

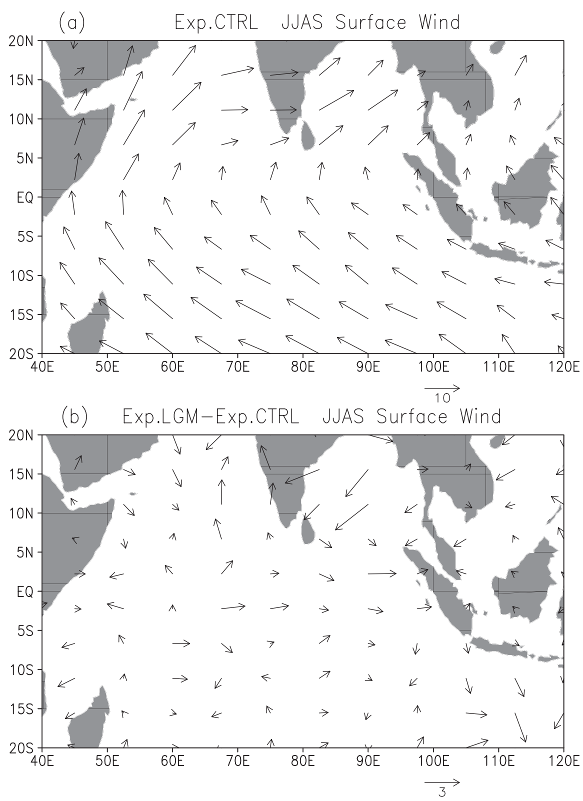

Fig. 6. Monsoon (JJAS) surface wind in (a) CTRL and (b) the difference between LGM and CTRL.

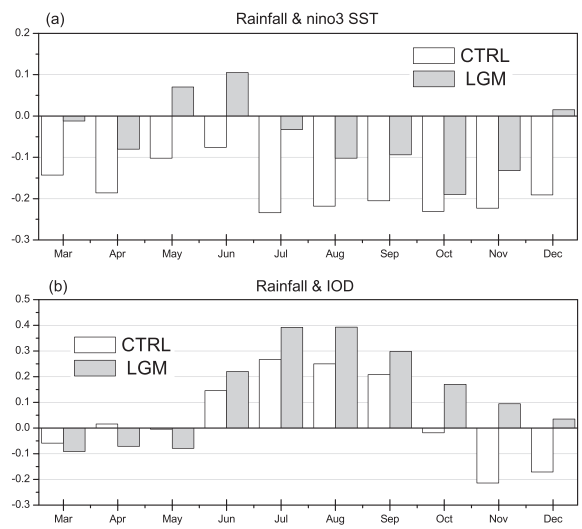

Fig. 7. The lagged correlation between South Asian monsoon rainfall (JJAS) with the monthly (a) Nino3 SST and (b) IOD index through the calendar year.

wind are increased considerably from 0.26 to 0.37, and from −0.40 to −0.48, respectively. These increases of correlation are statistically significant, with 95% confidence. Therefore, the glacial monsoon variability becomes almost independent of ENSO, but is correlated more with IOD. This opposite change of the monsoon correlation with ENSO and IOD can also be seen in the monthly correlation between the South Asia monsoon rainfall index (defined as the JJAS rainfall over South Asia, defined at the end of Section 3), and the monthly ENSO (Fig. 7a) and IOD (Fig. 7b) indices. Monsoon rainfall is negatively correlated with Nino3 SST during almost the entire year in the control, but the correlation is reduced greatly and even exhibits the opposite sign in LGM, with the negative correlation reduced most from July to September (Fig. 7a). In contrast, the positive correlation between monsoon rainfall and IOD increases clearly in the summer from July to September (Fig. 7b). Therefore, the reduction of the monsoon correlation with ENSO is highly likely to be distorted by the influence of the IOD. Interestingly, the opposite change of monsoon-ENSO correlation, and monsoon-IOD correlation simulated at glacial time is reminiscent of a similar interdecadal shift in recent decades: the monsoon-ENSO correlation

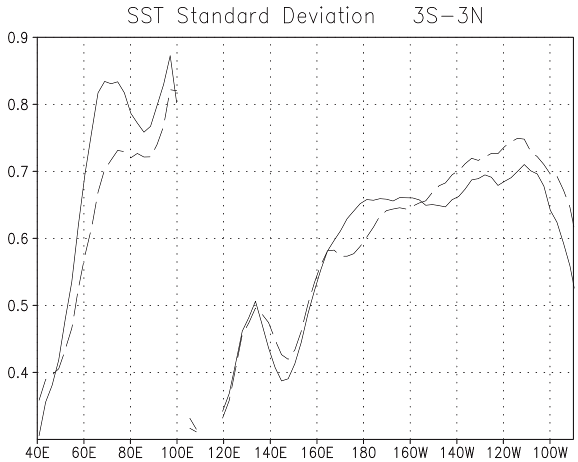

Fig. 8. Standard deviation of tropical SST anomaly across the Indian and Pacific for CTRL (solid) and LGM (dash).

decreases dramatically after 1980s, at the time when the monsoon-IOD correlation increases dramatically (Ashok et al. 2001).

The reduced correlation of Asian monsoon with ENSO is not caused by a reduction of ENSO variability at glacial times. Indeed, ENSO variability in LGM is largely unchanged, or even increased slightly, compared with the present, as seen in the standard deviations of the equatorial SSTs in the two simulations (Fig. 8). The increased ENSO activity appears to be consistent with a recent LGM simulation in NCAR CCSM1 (Otto-Bliesner et al. 2003).

Over the Indian Ocean, the IOD events become more distinctive, although the total SST variability is reduced slightly (Fig. 8). Indeed, the IOD now emerges as the 1st EOF of the tropical Indian Ocean SST (Fig. 1b), with the pattern virtually identical to that in CTRL (Fig. 1a), but the explained variance increased from 19% to 26%. The more distinct IOD can also be seen in the slightly enhanced subsurface temperature change (Fig. 3b), in comparison with the CTRL (Fig. 3a). As a result, the absolute amplitude of the 25 strongest IOD events remains comparable in the two simulations (Figs. 4a, b), with the glacial IOD extending 1–2 months longer into early winter. If we include all the IOD events (defined as the magnitude of IOD index larger than 0.3°C), the mean amplitude of the IOD events are even enhanced about 15% at LGM than at present (not shown). The occurring frequency of all the IOD events also increased substantially, as shown in Fig. 5. The reduced Indian Ocean SST variance is likely to be caused by the reduction of the overall Asian monsoon variability discussed before, because the surface heat flux associated with the monsoon variability is the major driving force of the SST variability over the Indian Ocean.

The first question is therefore why IOD remains strong, while overall SST variability is reduced over the Indian Ocean? This is a difficult question because our understanding of the mechanism that controls the strength of IOD is still limited. Li et al. (2003) presented a most comprehensive mechanism study for IOD. They proposed four mechanisms, including the tropical surface flux feedback, the anomalous anticyclone west over the Southeast Indian Ocean off the Sumatra coast, and the change of thermocline depth. We have analyzed these mechanisms. Our analysis suggests that the relative enhancement of IOD in LGM is most likely to be caused by the change of the tropical Indian Ocean thermocline, which in turn is caused by the weakening of the Asian monsoon at glacial times. As pointed out by Li et al. (2003), the tropical Indian Ocean thermocline is important for the generation of the IOD. An initial IOD event, say, in the positive phase (cold east and warm west), induces a westward surface pressure gradient force, that generates an easterly wind along the equator; this easterly then forces a downwelling Ekman pumping off the equator due to the anticyclonic wind curl and the change of the Coriolis force. This downwelling Ekman pumping generates downwelling Rossby waves off the equator traveling westward, which tends to further reinforce the initial warm SST in the west and therefore forms a positive feedback. In the mean time, an upwelling Kelvin wave is excited and propagates eastward, and then, after reflection, propagates westward as upwelling Rossby waves to form a delayed negative feedback. Since the tropical thermocline in the Indian Ocean shallows towards the west, this downwelling Rossby wave affects the SST most strongly in the west, especially south of the equator (Xie et al. 2002), overwhelming the negative feedback from the reflected waves formed in the eastern ocean.

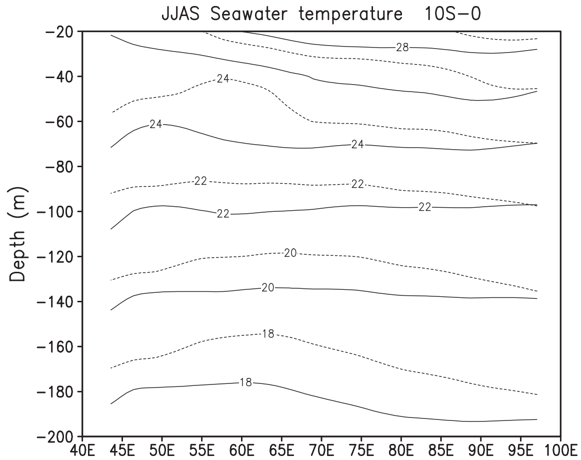

Fig. 9. Subsurface temperature in the tropical Indian Ocean (10°S–0° average) for CTRL (solid) and LGM (dash).

At LGM, from summer to fall, the weakened monsoon wind induces a westerly wind anomaly along the equator (Fig. 6b), which forces a mean upwelling in the wes and downwelling in the east, resulting in a tropical thermocline that shallows more in the west than in the east, especially near the surface layer (Fig. 9). For example, the 24°C isotherm shallows by 30-m in the west at about 55°E, but it shallows less than 10-m in the east (east of 90°E). Therefore, thermocline upwelling water is much more efficient to affect the SST, and in turn forms the positive feedback, in the west because of the significantly shallower thermocline, while the delayed negative feedback may remain relatively less changed because of the largely unchanged thermocline in the east. As a result, the IOD should be intensified. This intensified ocean-atmosphere feedback due to the shallower mean thermocline at LGM seems to be consistent with a lagged regression analysis of the upper ocean heat content with the IOD index (not shown). A definite conclusion of the mechanism of the IOD changes, however, would require much additional sensitivity experiments, which is beyond the scope of this paper.

The next question is why the Asian monsoon correlation is reduced with ENSO, but increased with IOD at LGM. The enhanced IOD discussed above naturally leads one to speculate the role of IOD as follows. The enhanced IOD has a stronger effect in enhancing the Asian monsoon rainfall, as seen in the composite IOD wind and precipitation in Fig. 2b, and then leads to an enhanced correlation of the Asian monsoon with the local IOD. The enhanced influence from IOD on monsoon, may then reduce the monsoon correlation with the ENSO. In the same time, the changed correlation between monsoon and climate variability can also be attributed to the change of the mean state. For example, the overall colder climate reduces the efficiency of latent heat release over the tropical Pacific ENSO region (even for the same magnitude of SST variability), which may weaken the teleconnection into South Asia, reducing the monsoon correlation with ENSO. On the Indian Ocean side, at LGM the weakened monsoon also exhibits a slight southward migration in its summer precipitation center. This southward migration of the Asian monsoon may be favorable for the IOD to affect the monsoon, and therefore enhancing the correlation between the two. A further study, however, is needed to quantify the relative contributions of each mechanism.

5. Summary

Our coupled model simulations suggest that at glacial times, the weakened Asian monsoon climatology results in a shallower tropical thermocline in the central-western Indian Ocean, which intensifies the ocean-atmosphere feedback and tends to enhance the IOD, relative to the background variability. The increased IOD exerts a stronger affect on South Asian monsoon, which may have led to a reduction of the monsoon correlation with ENSO. This opposite change of the monsoon-ENSO correlation to that of monsoon-IOD may be operating in other times. Although, currently, there is no relevant paleo-observation to compare with our current modeling work, by the nature of the modeling study here, this work is an attempt to stimulate further paleo-observational studies that search for the evidence of paleo-monsoon variability, and its relation with tropical climate variability modes.

Acknowledgments

We are grateful to three anonymous reviewers for their critical and insightful comments. All numerical experiments were performed on the supercomputer facility at the NCAR. This work is supported jointly by the US NSF, China's "973" Program (2004CB720208) and NSFC (40472086).

This work is CCR contribution No. 895.

References

Allan, R. and coauthors, 2001: Is there an Indian Ocean dipole, and is it independent of the El Niño-Southern Oscillations? *CLIVAR Exch.*, **6**(21), 18–22.

An, Z.S., X.H. Wu, P.X. Wang, S.M. Wang, G.R. Dong, X.J. Sun, D.E. Zhang, Y.Z. Lu, S.H. Zheng, and S.L. Zhao, 1991: Paleomonsoon of China over the last 130,000 years. *Science in China, Series B*, **34**, 1007–1024.

Anderson, D.M. and W.L. Prell, 1993: A 300 kyr record of upwelling off Oman during the late Quaternary: evidence of the Asian southwest monsoon. *Paleoceanography*, **8**, 193–208.

Ashok, K., Z. Guan, and T. Yamagata, 2001: Impact of the Indian Ocean dipole on the relationship between the Indian monsoon rainfall and ENSO. *Geophys. Res. Lett.*, **28**, 4499–4502.

Ashok, K., Z. Guan, and T. Yamagata, 2003: A look at the relationship between the ENSO and the Indian Ocean dipole. *J. Meteor. Soc. Japan*, **81**, 41–56.

Ashok, K., Z. Guan, N.H. Saji, and T. Yamagata, 2004: Individual and combined influences of ENSO and Indian Ocean Dipole on the Indian summer monsoon. *J. Climate*, **17**, 3141–3155.

Baquero-Bernal, A., M. Latif, and S. Legutke, 2002: On dipolelike variability of sea surface temperature in the tropical Indian Ocean. *J. Climate*, **15**, 1358–1368.

Behera, S.K. and T. Yamagata, 2003: Influence of the Indian Ocean Dipole on the Southern Oscillation. *J. Meteor. Soc. Japan*, **81**, 169–177.

Behera, S.K., S.A. Rao, H.N. Saji, and T. Yamagata, 2003: Comments on "A cantionary note on the interpretation of EOFs". *J. Climate*, **16**, 1087–1093.

Dong, B. and P.J. Valdes, 1998: Simulations of the Last Glacial Maximum climates using a general circulation model: prescribed versus computed sea surface temperatures. *Clim. Dyn.*, **14**, 571–591.

Guan, Z., K. Ashok, and T. Yamagata, 2003: Summertime response of the tropical atmosphere to the Indian Ocean dipole sea surface temperature anomalies. *J. Meteor. Soc. Japan*, **81**, 533–561.

Jacob, R., 1997: Low frequency variability in a simulated atmosphere ocean system. (Ph.D. thesis, University of Wisconsin-Madison.) 155 pp.

Ju, J. and J. Slingo, 1995: The Asian summer monsoon and ENSO. *Quart. J. Roy. Meteor. Soc.*, **121**, 1133–1168.

Krishnamurthy, V. and B.N. Goswami, 2000: Indian Monsoon—ENSO relationship on interdecadal time scales. *J. Climate*, **13**, 579–595.

Kumar, K.K., B. Rajagopalan, and M.A. Cane, 1999: On the weakening relationship between the Indian monsoon and ENSO. *Science*, **284**, 2156–2159.

Kutzbach, J.E. and P.J. Guetter, 1986: The influence of changing orbital parameters and surface boundary conditions on climate simulations for the last 18,000 years. *J. Atmos. Sci.*, **43**, 1726–1759.

Latif, M., K. Sperber, J. Arblaster, and P. Braconnot, 2001: ENSIP: the El Niño simulation intercomparison project. *Clim. Dyn.* **18**, 255–276.

Lau, N.-C. and M.J. Nath, 2004: Coupled GCM simulation of atmosphere-ocean variability associated with zonally asymmetric SST changes in the tropical Indian Ocean. *J. Climate*, **17**, 245–265.

Li, T., B. Wang, C.P. Chang, and Y. Zhang, 2003: A theory for the Indian Ocean dipole-zonal mode. *J. Atmos. Sci.*, **60**, 2119–2135.

Liu, Z. and H. Yang, 2003: Extratropical control on tropical climate: atmospheric bridge and oceanic tunnel. *Geophys. Res. Lett.*, **30**, 10.1029/2002GL016492.

Liu, Z., J. Kutzbach, and L. Wu, 2000: Modeling climatic shift of El Niño variability in the Holocene. *Geophys. Res. Lett.*, **27**, 2265–2268.

Liu, Z., B. Otto-Bliesner, J. Kutzbach, L. Li, and C. Shields, 2003: Coupled climate simulations of the evolution of global monsoons in the Holocene. *J. Climate*, **16**, 2472–2490.

Otto-Bliesner, B., E. Brady, S. Shin, Z. Liu, and C. Shields, 2003: Modeling El Niño and its tropical teleconnections during the glacial-interglacial cycle. *Geophys. Res. Lett.*, **30**, No. 23, 2198, doi:10.1029/2003GL08553.

Peltier, W.R., 2004: Global glacial isostasy and the surface of the ice-age Earth: the ICE-5G (VM2) model and GRACE. *Ann. Rev. Earth Planet. Sci.*, **32**, 111–149.

Saji, N.H., B.N. Goswami, P.N. Vinayachandran, and T. Yamagata, 1999: A dipole mode in the tropical Indian Ocean. *Nature*, **401**, 360–363.

Saji, N.H. and T. Yamagata, 2003: Structure of SST, surface wind variability during Indian Ocean Dipole mode events: COADS observations. *J. Climate*, **16**, 2735–2751.

Shin, S.I., Z. Liu, B.L. Otto-Bliesner, E.C. Brady, J.E. Kutzbach, and S.P. Harrison, 2003: A simulation of the Last Glacial Maximum climate using the NCAR CSM. *Clim. Dyn.*, **20**, 127–151.

Shukla, J., 1987: Interannual variability of monsoons. In *Monsoons*, edited by J.S. Fein and P.L. Stephens, John Wiley and sons, 399–464.

Shukla, J. and D.A. Paolino, 1983: The Southern Oscillation and long range forecasting of the summer monsoon rainfall over India. *Mon. Wea. Rev.*, **111**, 1830–1837.

Tokinaga, H. and Y. Tanimoto, 2004: Seasonal transition of SST anomalies in the tropical Indian Ocean during El Niño and Indian Ocean Dipole years. *J. Meteor. Soc. Japan*, **82**, 1007–1018.

Wang, B., S.C. Clements, and P. Liu, 2003: Contrasting the Indian and East Asian monsoons: implications on geologic timescales. *Marine Geology*, **201**, 5–21.

Webster, P.J., V.O. Magana, T.N. Palmer, J. Shukla, R.A. Tomas, M. Yanai, and T. Yasunari, 1998: Monsoons: processes, predictability, and the prospects for prediction. *J. Geophys. Res.*, **193**, 14,451–14,510.

Webster, P.J., A.M. Moore, J.P. Loschnigg, and R.R. Leben, 1999: Coupled ocean-atmosphere dynamics in the Indian Ocean during 1997–98. *Nature*, **401**, 356–360.

Wu, R. and B.P. Kirtman, 2004: Impacts of the Indian Ocean on the Indian summer monsoon-ENSO relationship. *J. Climate*, **17**, 3037–3054.

Xie, S.P., H. Annamalai, F.A. Schott, and J.P. McCreary, 2002: Structure and mechanisms of South Indian Ocean climate variability. *J. Climate*, **15**, 864–878.

Zhao, Y., P. Braconnot, O. Marti, S.P. Harrison, C. Hewitt, A. Kitoh, Z. Liu, U. Mikolajewicz, B. Otto-Bliesner, and S.L. Weber, 2005: A multi-model analysis of ocean feedback on the African and Indian monsoon during the mid-Holocene. *Clim. Dyn.*, **25**, 777–800.